

**Document Version**

Final published version

**Citation (APA)**

Abbas, Y., Deader, F. A., Abunahla, H., Baker, M., & Rezeq, M. (2023). Carbon Nanotubes Dispersion for Humidity Sensor Devices. In *2023 IEEE 23rd International Conference on Nanotechnology, NANO 2023* (pp. 325-328). (Proceedings of the IEEE Conference on Nanotechnology; Vol. 2023-July). IEEE.  
<https://doi.org/10.1109/NANO58406.2023.10231282>

**Important note**

To cite this publication, please use the final published version (if applicable).  
Please check the document version above.

**Copyright**

In case the licence states "Dutch Copyright Act (Article 25fa)", this publication was made available Green Open Access via the TU Delft Institutional Repository pursuant to Dutch Copyright Act (Article 25fa, the Taverne amendment). This provision does not affect copyright ownership.  
Unless copyright is transferred by contract or statute, it remains with the copyright holder.

**Sharing and reuse**

Other than for strictly personal use, it is not permitted to download, forward or distribute the text or part of it, without the consent of the author(s) and/or copyright holder(s), unless the work is under an open content license such as Creative Commons.

**Takedown policy**

Please contact us and provide details if you believe this document breaches copyrights.  
We will remove access to the work immediately and investigate your claim.

***Green Open Access added to TU Delft Institutional Repository***

***'You share, we take care!' - Taverne project***

**<https://www.openaccess.nl/en/you-share-we-take-care>**

Otherwise as indicated in the copyright section: the publisher is the copyright holder of this work and the author uses the Dutch legislation to make this work public.

# Carbon nanotubes dispersion for humidity sensor devices

Yawar Abbas, Firdous Ahmad Deader, Heba Abunahla, Mohammad Baker and Moh'd Rezeq

**Abstract**— Due to their stability, single-walled carbon nanotubes (SWCNTs) have been used for multiple applications in the semiconductor industry. Herein, we report the humidity sensing capability of SWCNTs by comparing the different densities of SWCNTs dispersed on the sensing area of the planner sensor device. Three different humidity sensors have been fabricated by preparing three different densities of CNTs diluted in deionized water and drop cast on the channel of 100  $\mu\text{m}$  width between 2mm x 1mm gold electrodes. It is observed that for very low density and high density of SWCNTs sensing layer, the sensing behavior either lacks in the detection range and response time, respectively. However, we found the optimized density of SWCNTs in deionized water for a highly sensitive, fast, and high-range humidity sensor for the optimized density of SWCNTs in deionized water.

## I. INTRODUCTION

Gas sensors are compact analytical tools that deliver real-time and ongoing information on the presence of certain gases. Humidity sensors are widely used in many applications such as food quality monitoring, manufacturing and process control medical equipment, and so forth, where accurate and reliable water content measurements in various environments and materials are essential. Owing to the size-dependent physical and chemical characteristics of nanomaterials, like nanoparticles [1-5], quantum dots [6, 7] and nanowires [8, 9], the research interest in these materials has been substantially increased. The resistive-based humidity sensors have been investigated extensively using polymer materials with less ability to detect humidity[10]. Due to the less sensitivity of carbon-based polymers, carbon nanotube (CNT)-based sensors have been developed.

The excellent electrical and mechanical properties of the CNTs and their ability to functionalize and integrate with electrical circuits make them the best choice for the sensing materials in humidity sensors. CNTs are cylindrical-shaped structures made up of carbon atoms that are arranged in a unique way. CNTs are known for their extraordinary properties, including high strength, electrical conductivity, and thermal conductivity. There are two main types of CNTs: single-walled carbon nanotubes (SWCNTs) [11] and multi-walled carbon nanotubes (MWCNTs)[12]. Single-walled carbon nanotubes (SWCNTs) are made up of a single layer of carbon atoms that are arranged in a cylindrical shape. They have a diameter of only a few nanometers but can be several micrometers long. SWCNTs are known for

their unique electronic properties, which are highly dependent on their diameter and chirality. Depending on their diameter and chirality, they can be either metallic or semiconducting. Due to their unique electrical and mechanical properties, SWCNTs have great potential for use in nanoelectronics[13, 14], nanoelectromechanical systems, and nanocomposites. MWCNTs are composed of multiple graphene sheets rolled into concentric cylinders. The layers are separated by about 0.34 nanometers, which is the distance between adjacent graphene sheets. MWCNTs can be either open-ended or closed-ended, depending on how they are synthesized. They have a larger diameter than SWCNTs, typically ranging from 2 to 100 nanometers, and can be several micrometers long. MWCNTs have excellent mechanical properties and are very strong, making them ideal for use in composites and reinforcing materials. SWCNTs and MWCNTs have unique properties that make them attractive for various applications. However, SWCNTs are more expensive to produce than MWCNTs, and their properties can vary significantly depending on their diameter and chirality. MWCNTs are easier to synthesize and have more consistent properties, making them more attractive for large-scale production. However, MWCNTs are more prone to defects and impurities due to the larger number of layers, which can affect their properties. Overall, both SWCNTs and MWCNTs have tremendous potential for use in various applications, including electronics, energy storage, sensors, and composites. Researchers continue to explore new ways to synthesize and manipulate these materials to take advantage of their unique properties and unlock their full potential.

In this work, we explore the humidity-sensing capacity of the SWCNTs by drop-casting them in different densities in the sensing area of the planer device. The sensor characteristics like response time, recovery time, dynamic response and humidity sensing range are observed to depend exclusively on the density of the SWCNTs film in the sensing area.

## II. EXPERIMENTAL PROCEDURE

The highly dense water-dispersed SWCNTs diameter of  $\sim 10$  nm and length of 3  $\mu\text{m}$  are purchased from US Research Nanomaterials, Inc to investigate the effect of SWCNTs density on humidity sensing. Three different densities of CNT solutions were prepared by adding 0.2 mL, 0.4 mL and 0.6 mL from the original solution in 50 mL of deionized (DI)

Research supported by and System on Chip Lab, Khalifa University of Science and Technology.

Yawar Abbas is the corresponding author and with Department of Physics and System on chip lab, Khalifa University, 127788, Abu Dhabi, UAE, yawar.abbas@ku.ac.ae.

Firdous Ahmad Deader is with Department of Physics and System on chip lab, Khalifa University, 127788, Abu Dhabi, UAE.

Heba Abunahla is with Quantum and Computer Engineering Department, Delft University of Technology, Delft, Netherlands.

M. Baker is with Department of Electrical and Computer Engineering and System on Chip Lab at Khalifa University, 127788, Abu Dhabi, UAE.

Moh'd Rezeq is with Department of Physics and System on chip lab, Khalifa University, 127788, Abu Dhabi, UAE.

water. The highly cleaned cyclic olefin copolymer (COC) substrate was prepared by rinsing it with deionized water. Then it was washed with isopropyl alcohol for 15 min and acetone for the same duration using a sonicator. The substrate was further dried with the help of an  $N_2$  gun. After cleaning the COC substrate, the Au thin film of around 200 nm was deposited using the DC magnetron sputtering. The positive photoresist is spin-coated on the Au-coated COC substrate, and the 2 mm x 1mm patterns with 100  $\mu$ m spacing is designed with the help of a laser writer. Followed by development, the etching process is carried out with the help of a gold etchant. The final substrate with the gold electrodes with 100  $\mu$ m spacing between them is prepared in this fabrication. Finally, the different density CNTs were dropped cast in a 100  $\mu$ m channel to test the humidity sensing of the devices. The dispersion density of SWCNTs in the channel is confirmed with the help of a Field Emission Electron Microscope (FESEM). The impedance of the devices was monitored with the use of an LCR meter in different humidity environments. To prepare the targeted humidity environment the saturated salt solutions of  $K_2SO_4$ , KCl, NaCl, NaBr,  $MgCl_2$ ,  $C_2H_3KO_2$  and NaOH salts in DI water are prepared in half of the glass jars, and the lid of the jar is kept closed. Allow time for humidity to stabilize by observing the humidity values using a standard humidity sensor. We adjusted the humidity by adding more salt for higher levels or DIwater for lower levels. In this way, we prepared the relative humidity of 97%, 86%, 75%, 57%, 33%, 22%, and 6%.

### III. RESULTS AND DISCUSSIONS

Figure 1 shows the schematic diagram of the complete sensor fabrication process and the set-up for measuring humidity measurements. Figure 1 (a) shows the device fabrication schematics of the humidity sensor.

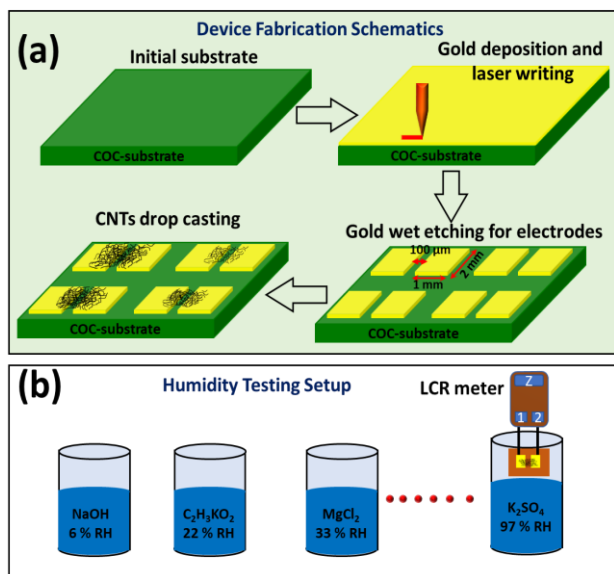


Figure 1. (a) The complete fabrication flow of the humidity sensor and (b) the schematic diagram of the humidity measurement test.

Au thin film of 200 nm is deposited on the COC substrate, and the electrode pattern is designed using a laser writer on the positive photoresist.

The Au thin film is etched using the standard potassium iodide solution to obtain the 2 mm x 1 mm standard electrodes with a spacing between them of 100  $\mu$ m, as shown in Fig. 1 (a). Finally, the different concentrations of SWCNT solution are drop cast between the electrodes to obtain the complete humidity sensor, as shown in Fig. 1 (a). Figure 1 (b) depicts the humidity measurement set up for the sensor in which the different humidity environments in closed chambers are generated with the help of different salt solutions.

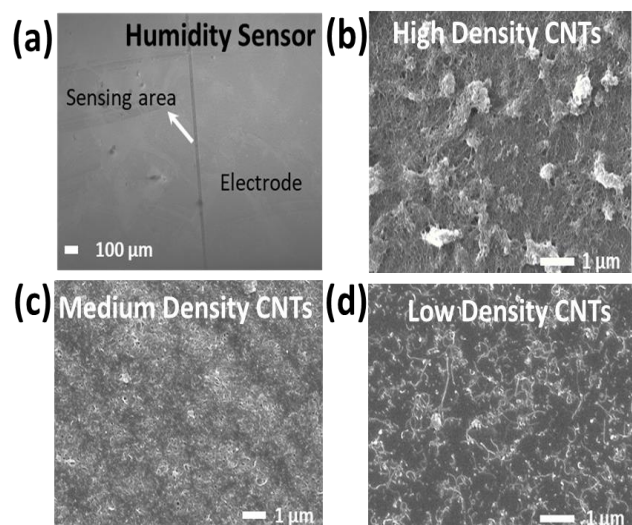


Figure 2. The SEM micrographs of (a) humidity sensor, (b) dispersion of high-density drop cast CNTs, (c) medium-density drop cast CNTs and (d) low-density drop cast CNTs.

The standard humidity set-up is prepared by the  $K_2SO_4$ , KCl, NaCl, NaBr,  $MgCl_2$ ,  $C_2H_3KO_2$  and NaOH salt solutions with the relative humidity of 97%, 86%, 75%, 57%, 33%, 22%, and 6% respectively.

The fabricated devices are further carried out for the SEM analysis. Figure 2 shows the SEM micrographs of the device and magnification images of SWCNTs dispersion in the sensing region of the sensors.

Figure 2 (a) shows a clear image of the 100  $\mu$ m sensing area between the Au electrodes, whereas, Fig. 2 (b), (c) and (d) shows the highly dense, monodispersed and low dense SWCNTs in the sensing area of the sensor, respectively.

After confirming the distribution of SWCNTs in the sensing area of the humidity sensors, the devices are tested to investigate their sensitivity in different relative humidity (RH) levels. The percentage RH (% RH) is measured with the help of a standard humidity sensor in this experiment. Figure 3 shows the initial test of the humidity sensors in which the impedance of the devices is measured by exposing them to the humidity with the help of the commercially available humidifier, and the impedance of the devices is measured at different humidity levels. Figure 3 (a), (b) and (c) shows the sensitivities of sensors when exposed to constant humidity periodically. It is observed that the impedance of all devices increases when exposed to standard humidity periodically, but a clear drift in impedance (increase) is observed as compared to its previous value.

An increase in humidity causes the impedance of all humidity sensors to increase due to the adsorption of water molecules onto the SWCNT surface. As the sensor is exposed to humid air, the water molecules are adsorbed onto the CNTs, leading to an increase in the interfacial resistance, also known as the charge-transfer resistance. In addition, the adsorbed water molecules act as a dielectric material, and the thickness of the dielectric layer increases with an increase in humidity. This, in turn, causes a decrease in electrical conductance between the SWCNTs, resulting in an increase in impedance, which can be measured and calibrated to measure humidity accurately.

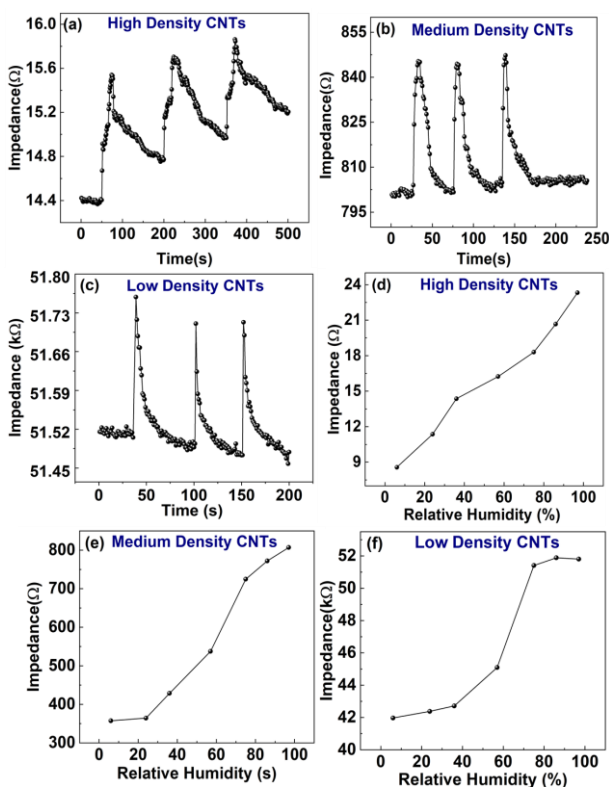


Figure 3. The dynamic response curves of the sensors with (a) high-density CNTs, (b) medium-density CNTs and (c) low-density CNTs in the channel, whereas (d), (e) and (f) show the impedance response of high, medium and low humidity sensors, respectively.

The SWCNT humidity sensor's impedance change is influenced by various factors, such as the diameter and length of the SWCNTs, the type of metal used as electrodes, and the thickness of the SWCNT film. Therefore, the sensor's sensitivity can be enhanced by optimizing these parameters and employing appropriate functionalization of the SWCNTs. Overall, the CNT humidity sensor's increase in impedance with an increase in humidity results from the adsorption of water molecules on the CNT surface, which has made it possible to develop highly sensitive and selective humidity sensors based on CNTs. Figure 3 (d), (e) and (f) the impedances of the sensors for the % RH of 97%, 86%, 75%, 57%, 33%, 22%, and 6%. Interestingly, the high-density CNT-based sensor exhibited the full range sensitivity, whereas the ranges of medium and low-density CNT-based sensors were 20 % ~100 % and 35 % ~75 %, respectively.

Finally, the transient response of the impedance of all sensors is investigated by inserting the sensor in the 97 % humidity from the atmospheric humidity, i.e. 36% and monitoring its change in impedance with time, as shown in Figure 4. The impedance response time for the high-density, medium-density and low-density CNTs-based sensors are calculated as 200 s, 15 s and 4 s, respectively. At the same time, the recovery time for the high-density, medium-density and low-density CNTs-based sensors are calculated as 300 s, 146 s and 53 s, respectively, calculated from Fig. 4 (a), (b) and (c).

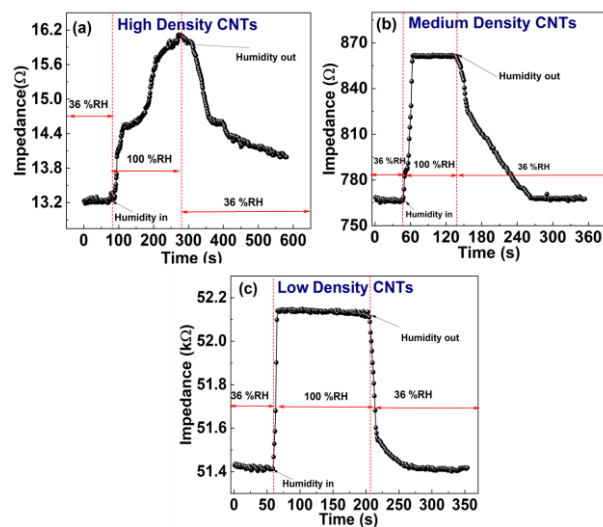


Figure 4. The transient response and recovery curves of humidity sensors based on (a) high-density CNTs, (b) medium-density CNTs and (c) low-density CNTs.

From Fig. 3 and 4, it can be clearly seen that the high-density CNT-based sensor has a very long response and recovery time, and there is drift in its impedance when it is exposed to maximum humidity periodically. On the other hand, in the case of a low-density-based sensor, their response and recovery time are faster than medium-density CNTs, but it has a very poor humidity sensing range of 35 % ~75 %. Hence, if one compromised on the slightly less response and recovery time of a medium-density CNTs-based sensor, it is obvious that the monodispersed CNTs-based sensor is the best candidate for practical applications with the nearly linear range of 20% ~100 %.

#### IV. CONCLUSION

In conclusion, we designed and investigated a humidity sensor based on CNTs. Different CNTs densities, as a sensing layer, were dispersed between two Au electrodes separated by 100  $\mu\text{m}$  width. The high, medium, and low densities of CNTs in the sensing area of the humidity sensor are confirmed with the help of SEM micrographs. It is observed that the high density of CNTs in the sensing of the sensor gave us the full range of the humidity. Still, its response and recovery times were very high, i.e. 200 s and 300 s, respectively, which is not preferable for humidity sensors. Compared to medium-density CNTs, a low-density-based sensor responds and recovers more rapidly.

Nevertheless, its 35%–75% humidity detecting range is incredibly inadequate. Because of its monodispersed nature and virtually linear sensing range of 20%–100%, a medium-density CNTs-based sensor is preferable for practical applications if one is ready to accept slightly slower response and recovery times.

#### ACKNOWLEDGMENT

This publication is based on work supported by System on Chip Lab, Khalifa University of Science and Technology.

#### REFERENCES

- [1] L. Y. Chou and W. C. Chan, "Fluorescence-tagged gold nanoparticles for rapidly characterizing the size-dependent biodistribution in tumor models," *Advanced healthcare materials*, vol. 1, no. 6, pp. 714-721, 2012.
- [2] C. Rao, G. Kulkarni, P. J. Thomas, and P. P. Edwards, "Size-dependent chemistry: properties of nanocrystals," *Chemistry—A European Journal*, vol. 8, no. 1, pp. 28-35, 2002.
- [3] Y. Abbas, M. Rezeq, A. Nayfeh, and I. Saadat, "Size dependence of charge retention in gold-nanoparticles sandwiched between thin layers of titanium oxide and silicon oxide," *Applied Physics Letters*, vol. 119, no. 16, p. 162103, 2021.
- [4] A. Rezk, Y. Abbas, I. Saadat, A. Nayfeh, and M. Rezeq, "Charging and discharging characteristics of a single gold nanoparticle embedded in Al<sub>2</sub>O<sub>3</sub> thin films," *Applied Physics Letters*, vol. 116, no. 22, p. 223501, 2020.
- [5] Y. Abbas, A. Rezk, S. Anwer, I. Saadat, A. Nayfeh, and M. Rezeq, "Improved figures of merit of nano-Schottky diode by embedding and characterizing individual gold nanoparticles on n-Si substrates," *Nanotechnology*, vol. 31, no. 12, p. 125708, 2020.
- [6] J. Gao, J. M. Luther, O. E. Semonin, R. J. Ellingson, A. J. Nozik, and M. C. Beard, "Quantum dot size dependent J–V characteristics in heterojunction ZnO/PbS quantum dot solar cells," *Nano letters*, vol. 11, no. 3, pp. 1002-1008, 2011.
- [7] M. Rezeq, Y. Abbas, B. Wen, Z. Wasilewski, and D. Ban, "Direct detection of electronic states for individual indium arsenide (InAs) quantum dots grown by molecular beam epitaxy," *Applied Surface Science*, vol. 590, p. 153046, 2022.
- [8] R. Calarco *et al.*, "Size-dependent photoconductivity in MBE-grown GaN–nanowires," *Nano letters*, vol. 5, no. 5, pp. 981-984, 2005.
- [9] Y. Wen, Y. Zhang, and Z. Zhu, "Size-dependent effects on equilibrium stress and strain in nickel nanowires," *Physical Review B*, vol. 76, no. 12, p. 125423, 2007.
- [10] M. A. Najeeb, Z. Ahmad, and R. A. Shakoor, "Organic thin-film capacitive and resistive humidity sensors: a focus review," *Advanced Materials Interfaces*, vol. 5, no. 21, p. 1800969, 2018.
- [11] S. Niyogi *et al.*, "Chemistry of single-walled carbon nanotubes," *Accounts of Chemical Research*, vol. 35, no. 12, pp. 1105-1113, 2002.
- [12] J. H. Lehman, M. Terrones, E. Mansfield, K. E. Hurst, and V. Meunier, "Evaluating the characteristics of multiwall carbon nanotubes," *Carbon*, vol. 49, no. 8, pp. 2581-2602, 2011.
- [13] L. Tizani, Y. Abbas, A. M. Yassin, B. Mohammad, and M. Rezeq, "Single wall carbon nanotube based optical rectenna," *RSC advances*, vol. 11, no. 39, pp. 24116-24124, 2021.
- [14] Y. Abbas, M. U. Khan, F. Ravoux, B. Mohammad, and M. Rezeq, "Focused Ion Beam Engineering of Carbon Nanotubes for Optical Rectenna Applications," *ACS Applied Nano Materials*, 2022.